Proceedings of the 19th World Congress
The International Federation of Automatic Control
Cape Town, South Africa. August 24-29, 2014

Errors-in-Variables identification in bilaterally coupled systems with application to oil well testing ⋆

Mehdi Mansoori *,**, **Arne Dankers** * and
Paul M.J. Van den Hof ***,*

* *Delft Center for Systems and Control, Delft University of Technology, Mekelweg 2, 2628 CD Delft, The Netherlands (email: {m.mansoorihabibabadi, a.g.dankers}@tudelft.nl)*
** *Chemical and Petroleum Engineering Department, Sharif University of Technology, Azadi St., Tehran, Iran*
*** *Department of Electrical Engineering, Eindhoven University of Technology, The Netherlands (email: p.m.j.vandenhof@tue.nl)*

Abstract: Bilaterally coupled models are a genuine tool for modeling interconnected physical systems. It is shown that identification problems in bilaterally coupled systems can be recast into a closed-loop identification problem. When all measured signals are subject to sensor noise a closed-loop errors-in-variables problem results, for which an attractive non-parametric and instrumental-variable solutions are presented. The developed methods are applied to an example from oil reservoir engineering, being the estimation of reservoir dynamics from measurements at the well bore.

Keywords: System identification, closed-loop identification, errors-in-variables method, instrumental variables, well testing, reservoir engineering.

1. INTRODUCTION

Many physical systems can effectively be described in the form of two-port systems or bilaterally coupled systems. Exchange of energy between different systems is then typically described by two physical variables that describe the interaction, see e.g. also port-Hamiltonian systems. Bilateral coupling of systems is also a general tool for describing concatenated systems as in transportation networks, and is currently also the main paradigm in dealing with decentralized and distributed control systems as reflected in Figure 1. Through bilateral couplings, systems can be connected to form large scale interconnected dynamic networks. In robust control problems, the considered system

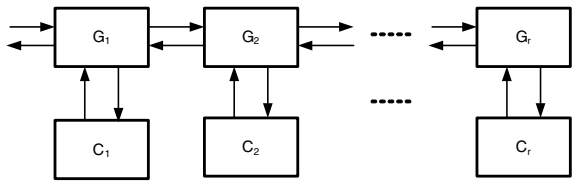

Fig. 1. Decentralized control system.

connections are often represented in the form of linear fractional transformations (LFT), which is fully equivalent to the bilaterally coupled form.

While state estimation and (distributed) control problems are now commonly addressed in this setting, problems of identification of the dynamic modules are mostly restricted to be analyzed in more simple system configurations, i.e. open-loop or closed-loop.

Identification in more complex structured dynamic networks has recently attracted more attention. In Materassi and Innocenti [2010], Sanandaji et al. [2011], Dankers et al. [2012] the problem of identifying the structure of a dynamic network has been addressed, while in Van den Hof et al. [2013], Dankers et al. [2013] the identification of particular dynamic modules (sub-systems) has been addressed for a known interconnection structure.

In this paper we will address the general identification problem for bilaterally coupled systems. It will appear that this identification configuration can be casted into a "classical" closed-loop identification setting, for which standard methods exist. However when the measured signals are all measured under the influence of (sensor) noise, an errors-in-variables (EIV) problem occurs, which in a closed-loop setting does not have easy and standard solutions. E.g. a so-called direct method for closed-loop identification will generally not provide consistent estimates if all measured variables are contaminated with sensor noise.

Here we will develop a non-parametric and an instrumental variable (IV) method that can solve the particular EIV-problem in closed-loop. Both methods have the advantage that they are algorithmically very simple.

The step from bilaterally coupled system to a EIV-closed-loop configuration is illustrated for the case of a well-testing situation in oil reservoir engineering, where mea-

⋆ The work of Arne Dankers is supported in part by the National Science and Research Council (NSERC) of Canada and the work of Mehdi Mansoori is supported in part by Dana Energy Company.

sured well pressures and flows are used to identify characteristics of the underlying oil reservoir. This example is cast into the described EIV setting, and identification results are shown to illustrate the presented identification method.

The rest of the paper is structured as follows. First bilaterally coupled systems are introduced and cast into an identification framework. Then the generalized nonparametric and IV methods are presented to handle the related EIV-identification problem. Subsequently a well test example is given to illustrate the results.

2. IDENTIFICATION IN BILATERALLY COUPLED SYSTEMS

The system setup that we consider in this paper is reflected in Figure 2, composed of two inputs u_1, u_2 and two outputs y_1, y_2, where the output signals are contaminated with additive disturbance signals v_1, v_2, being realizations of stationary stochastic processes. Identification of the linear time-invariant components G_{ji}, $i, j = 1, 2$ on the basis of measured data u_1, u_2 and y_1, y_2 is a standard multivariable open-loop identification problem.

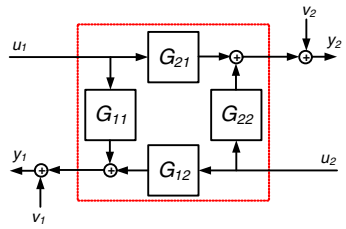

Fig. 2. System configuration in bilateral form.

When to of such systems get connected, as sketched in Figure 3, we can simply equate the signals at the connection node, i.e. $y_2 = u_3$ and $u_2 = y_3$, and a concatenated system occurs. Now the identification of particular transfers becomes more involved, in particular because of the "loop" that connects the transfers G_{22} and G_{33}. Several different identification problems can be formulated now. In this paper we will particularly focus on the problem of identifying G_{33} on the basis of measurements y_2, y_3 at the interconnection node. This transfer G_{33} can be interpreted as the load that is connected to the original system. To this

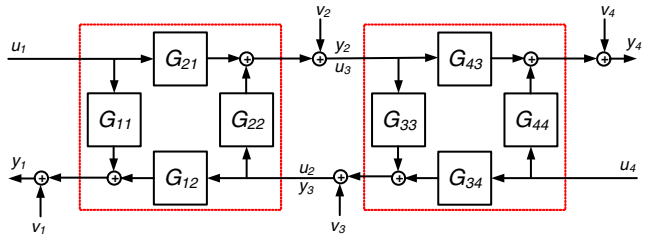

Fig. 3. Bilaterally coupled systems.

end we isolate the parts of the interconnected network that are relevant for the identification of G_{33} into the structure that is given in Figure 4. In this diagram we have removed the effect of y_1, while we have assumed that the port at node 4 is not connected to any other system (no load). The result is now a more or less standard closed-

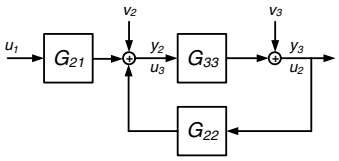

Fig. 4. Bilaterally coupled systems recast in closed-loop form for identification of G_{33}.

loop configuration where the to-be-identified object G_{33} is positioned in the forward path between u_3 and y_3, and where G_{22} acts as a feedback "controller". The additional input signal u_1 then can be given the interpretation of a reference signal.

For the identification of G_{33} on the basis of measured u_3, y_3 and possibly u_1 several closed-loop identification methods are available Ljung [1999], ranging from direct methods that only use measured signals u_3, y_3, to indirect methods that also utilize the "reference" signal u_1. Solutions for this problem are typically available when signals u_3, y_3 (and possibly u_1) can be measured free from measurement/sensor noise. In the next section we will focus on this identification problem for the situation that all measured signals are subject to sensor noise, turning the problem into an errors-in-variables problem.

3. CLOSED-LOOP ERRORS-IN-VARIABLES IDENTIFICATION

In this section the identification of a closed-loop system is considered where noisy measurements of the input, output and reference are available. The identification setup is shown in Fig. 5.

This is can be seen as an extension of the open loop Errors-in-Variables (EIV) framework to a closed-loop setting. The open loop EIV identification problem has been extensively studied (a survey paper is Söderström [2012]). In general, given only noisy measurements of the input and output of a system operating in open loop, the dynamics of the plant are not identifiable. Using some prior knowledge, the problem may become identifiable [Söderström, 2012].

In Söderström et al. [2013] various closed-loop EIV data generating systems are considered. In all the systems investigated in that paper, a noise-free reference signal is assumed to be known. Thus, the case we study here is a slight generalization of that one.

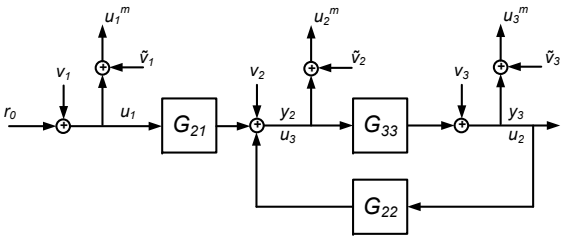

Fig. 5. Closed-loop data generating system with sensor noise

As in the open-loop case, the presence of the sensor noise does not have trivial consequences for the closed-loop

identification problem. In fact, none of the closed-loop identification methods presented in Forssell and Ljung [1999] will result in consistent estimates of the plant if there is sensor noise on either the input and/or the reference.

In the following subsections, two methods are presented to obtain estimates of G_{33}. First a non-parametric method is presented. It is based on obtaining an estimate of the cross power spectral densities of the data. Secondly, a (parametric) instrumental variable (IV) method is presented. Before studying the methods, the data generating system is formalized.

3.1 Closed-Loop Errors-in-Variables System

The equations for the system shown in Fig. 5 are:

$$y_2(t) = G_{21}(q)u_1(t) + G_{22}(q)u_2(t) + v_2(t)$$
$$y_3(t) = G_{33}(q)u_3(t) + v_3(t)$$

where q denotes the shift operator (i.e. $q^{-1}u(t) = u(t-1)$) and each v denotes *process noise*, which is modeled by a stationary stochastic process with rational power spectral density. The variable u_1 is an *external variable*, usually referred to as the reference in control systems. It may possible to (indirectly) influence this variable. The variables u_1, u_2 and u_3 are measured with noise:

$$\tilde{u}_i(t) = u_i(t) + s_i(t),\ i = 1, 2, 3,$$

where s_1, s_2 and s_3 denote the *sensor noise* (or error), that is assumed to be a stationary stochastic process with rational power spectral density (it is not necessarily assumed to be white noise). Note that $\tilde{y}_3 = \tilde{u}_2$ and $\tilde{y}_2 = \tilde{u}_3$.

The transfer function G_{33} is assumed to be a rational function, i.e $G_{33}(q) = \frac{B^0_{33}(q)}{A^0_{33}(q)}$ where A^0_{33} and B^0_{33} are coprime polynomials in q.

The data generating system is assumed to satisfy the following conditions.

Assumption 1. Conditions on the noise.
The variables s_1, v_1 and r_0 are uncorrelated to the sensor noise s_2 and s_3, and process noise v_2 and v_3. [1] □

In the following two subsections it will be shown how to obtain estimates of G_{33} using only $\tilde{u}_1$, $\tilde{u}_2$, and $\tilde{u}_3$.

3.2 Non-Parametric Method

In this section it is shown that a non-parametric estimate of G_{33} can be obtained directly from the cross power spectral densities of the available signals. In particular, it is shown that

$$G_{33}(\omega) = \frac{\Phi_{\tilde{y}_3\tilde{u}_1}(\omega)}{\Phi_{\tilde{y}_2\tilde{u}_1}(\omega)} \tag{1}$$

where $\Phi_{\tilde{y}_3\tilde{u}_1}$ is the cross power spectral density of $\tilde{y}_3$ and $\tilde{u}_1$, and $\Phi_{\tilde{y}_2\tilde{u}_1}$ is the cross power spectral density of $\tilde{y}_2$ and $\tilde{u}_1$. This method is suggested in Söderström et al. [2013] for the case where u_1 is measured noise free. Here we show that the method works, even when a noisy measurement of u_1 is available.

[1] s_1 is uncorrelated to s_2 if the cross-correlation between s_1 and s_2, $R_{s_1s_2}(\tau)$ is zero for all τ.

The cross power spectral density of $\Phi_{\tilde{y}_3\tilde{u}_1}$ is the Discrete Time Fourier Transform of the cross-correlation of $\tilde{y}_3$ and $\tilde{u}_1$, which is equal to:

$$R_{\tilde{y}_3\tilde{u}_1}(\tau) = \bar{\mathbb{E}}[\tilde{y}_3(t)\tilde{u}_1(t-\tau)] \tag{2}$$

where $\bar{\mathbb{E}}[\cdot]$ denotes the expected value operator in a quasi-stationary framework and is defined as $\bar{\mathbb{E}} := \lim_{N\to\infty}\frac{1}{N}\sum_{t=0}^{N-1}\mathbb{E}$ and $\mathbb{E}$ is the expected value operator [Ljung, 1999]. Expressing $\tilde{y}_3$ in terms of u_1 results in:

$$R_{\tilde{y}_3\tilde{u}_1}(\tau) = \bar{\mathbb{E}}\Big[\Big(G_{33}(q)S(q)G_{21}(q)u_1(t) + S(q)G_{33}(q)v_2(t) + S(q)v_3(t) + s_3(t)\Big)\Big(u_1(t-\tau) + s_1(t-\tau)\Big)\Big] \tag{3}$$

where S denotes the sensitivity function $S = \frac{1}{1-G_{22}G_{33}}$. By Assumption 1, (3) can be simplified to:

$$R_{\tilde{y}_3\tilde{u}_1}(\tau) = \bar{\mathbb{E}}\big[G_{33}(q)S(q)G_{21}(q)u_1(t)\cdot u_1(t-\tau)\big] \tag{4}$$

Thus, by taking the Discrete Time Fourier Transform of (4) the cross power spectral density of $\tilde{y}_3$ and $\tilde{u}_1$ is:

$$\Phi_{\tilde{y}_3\tilde{u}_1}(\omega) = G_{33}(e^{j\omega})S(e^{j\omega})G_{21}(e^{j\omega})\Phi_{u_1}(\omega) \tag{5}$$

where $\Phi_{u_1}(\omega)$ is the power spectral density of u_1.

By the same reasoning, it can be shown that the cross power spectral density of $\tilde{y}_2$ and $\tilde{u}_1$ is:

$$\Phi_{\tilde{y}_2\tilde{u}_1}(\omega) = S(e^{j\omega})G_{21}(e^{j\omega})\Phi_{u_1}(\omega). \tag{6}$$

Thus it is clear from (5) and (6) that (1) holds.

An estimate of $\Phi_{\tilde{y}_2\tilde{u}_1}$ can be obtained using $\tilde{y}_2$ and $\tilde{u}_1$ by calculating the periodogram [Ljung, 1999]. Essentially this means an estimate of $\Phi_{\tilde{y}_2\tilde{u}_1}$ can be obtained using the Discrete Fourier Transform (DFT) of $\tilde{y}_2$ and $\tilde{u}_1$:

$$\hat{\Phi}^N_{\tilde{y}_2\tilde{u}_1}(\omega) = \frac{1}{N}\tilde{Y}_2(e^{j\omega})\tilde{U}_1(e^{-j\omega})$$

where $\tilde{Y}_2(e^{j\omega})$ and $\tilde{U}_1(e^{-j\omega})$ denote the N point DFT of N samples of $\tilde{y}_2$ and $\tilde{u}_1$ respectively.

In the signal processing and identification literature, periodograms are often smoothed using smoothing windows such as Bartlett or Hamming windows [Ljung, 1999].

In the following section a method is presented to obtain a parametric estimate of G_{33}.

3.3 Basic Closed-Loop Instrumental Variable Method

In the following text, the Basic Closed-Loop Instrumental Variable method of Gilson and Van den Hof [2005] will be presented. In Gilson and Van den Hof [2005] they suppose that noise free measurements of u_1, y_2 and y_3 are available. We show that even in the presence of sensor noise, the method still results in consistent estimates of G_{33}.

The model is a parameterized rational function:

$$G_{33}(q,\theta) = \frac{B_{33}(q,\theta)}{A_{33}(q,\theta)} = \frac{q^{-n_k}(b^{33}_0 + b^{33}_1 q^{-1} + \cdots + b^{33}_{n_b}q^{-n_b})}{1 + a^{33}_1 q^{-1} + \cdots + a^{33}_{n_a}q^{-n_a}}$$

where the parameter vector is $\theta = [a^{33}_1\ \cdots\ a^{33}_{n_a}\ b^{33}_0\ \cdots\ b^{33}_{n_b}]^T$. The following regressor will be very useful:

$$\phi^T_{33}(t) = [-\tilde{y}_3(t-1)\ \cdots\ -\tilde{y}_3(t-n_a)\ \tilde{u}_3(t)\ \cdots\ \tilde{u}_3(t-n_b)]$$

The output $\tilde{y}_3$ can now be expressed as

$$\begin{aligned}\tilde{y}_3(t) &= B^0_{33}(q)\tilde{u}_3(t) + \big(1 - A^0_{33}(q)\big)\tilde{y}_3(t) \\ &\quad - B^0_{33}(q)s_2(t) + A^0_{33}(q)\big(v_3(t) + s_3(t)\big) \\ &= \phi^T_{33}(t)\theta^0_{33} + \breve{v}_3(t)\end{aligned} \tag{7}$$

where B_{33}^0 and A_{33}^0 denote the true numerator and denominator of G_{33}, θ_{33}^0 denotes the true parameters, and

$$\breve{v}_3(t) = -B_{33}^0(q)s_2(t) + A_{33}^0(q)\big(v_3(t) + s_3(t)\big). \quad (8)$$

The IV estimate of θ_{33}^0 is defined as [Gilson and Van den Hof, 2005]

$$\hat{\theta}_{IV} = \text{sol}\Big\{\frac{1}{N}\sum_{t=0}^{N-1} z(t)\big(\tilde{y}_3(t) - \phi_{33}^T(t)\theta\big) = 0\Big\},$$

where $z(t)$ is a vector of so called *instruments*. If $\sum_{t=0}^{N-1} z(t)\phi_{33}^T(t)$ is nonsingular, then

$$\hat{\theta}_{IV} = \Big(\frac{1}{N}\sum_{t=0}^{N-1} z(t)\phi_{33}^T(t)\Big)^{-1}\Big(\sum_{t=0}^{N-1} z(t)\tilde{y}_3(t)\Big). \quad (9)$$

An expression of $\hat{\theta}_{IV}$ in terms of θ_0 can be obtained by substituting (7) into (9):

$$\hat{\theta}_{IV} = \theta^0 + \Big(\frac{1}{N}\sum_{t=0}^{N-1} z(t)\phi_{33}^T(t)\Big)^{-1}\Big(\sum_{t=0}^{N-1} z(t)\breve{v}_3(t)\Big). \quad (10)$$

Thus, $\hat{\theta}_{IV} \to \theta^0$ as $N \to \infty$ with probability 1 (i.e. it is *consistent*) if the following conditions hold:

(a) $\bar{\mathbb{E}}[z(t)\phi_{33}^T(t)]$ is nonsingular,
(b) $\bar{\mathbb{E}}[z(t)\breve{v}_3(t)] = 0$.

where $\bar{\mathbb{E}}[\cdot] = \lim_{N\to\infty}\frac{1}{N}\sum_{t=0}^{N-1}\mathbb{E}[\cdot]$ and $\mathbb{E}$ is the expected value operator [Ljung, 1999].

The choice of the instrumental variable z is critical with respect to the consistency of the estimates. Consider

$$z(t) = [\tilde{u}_1(t) \ \cdots \ \tilde{u}_1(t - n_a - n_b)]^T.$$

By Assumption 1 and (8), Condition (b) is met. Consequently, consistent estimates of G_{33} are possible using this instrument. Note that, by (9), in order to calculate the estimate $\hat{\theta}_{IV}$ only a linear regression needs to be evaluated.

In the following section, it is shown how the data generating system 5 could arise in a practical situation. Then both the parametric and non-parametric identification methods presented are applied to simulated data.

4. WELL TEST ANALYSIS

Well test analysis is the standard procedure to extract information about dynamic properties and geological features of an underground hydrocarbon reservoir from flow and pressure measurements. The test involves producing from a well based on a sequence of planned wellhead flow rates and recording the pressure and flow rate at the bottom hole of the well. Conventionally, either the step or impulse response of the reservoir is calculated by *deconvolution*. Then the impulse response (or step response) is used to estimate the physical parameters of the reservoir Gringarten [2008]. The well test analysis problem can be seen as a system identification which first a dynamical model is identified based on the measurements. Then, the identified model is utilized to estimate the physical parameters of the reservoir using the frequency responses of the physics based model and the identified model. Here, we only consider estimating the average permeability but estimation of other parameters such as skin factor can be included the proposed procedure. In order to apply the identification method the causal structure of the system needs to be known. Therefore in the following sections, first it is shown how the well and reservoir can be modeled as a bilaterally coupled system and the causal structure is derived. Then the identification methods of the previous sections are applied to a simulated data set. Finally the identified model is used to obtain an estimate of the permeability of the reservoir.

4.1 Modeling The Well Test Process

For simplicity, a homogeneous reservoir connected to the surface with a vertical well is considered. The production system is comprised a convective flow in the well bore and diffusive flow in the reservoir that interact with each other at the bottom hole of the well; see Fig. 6.

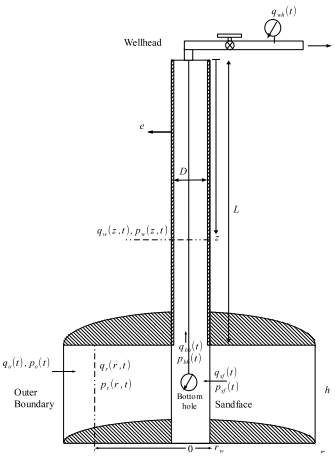

Fig. 6. A cylindrical homogeneous reservoir with a vertical well

The reservoir and well bore shown in Fig. 6 are modeled as two bilaterally coupled subsystems. First the equations for the well bore and then the reservoir are presented.

Consider modeling the well bore. The flow of a single-phase liquid in the well bore is governed by the water-hammer equations [Chaudhry, 1987]. Thus, the equations for the flow rate $q(z,t)$, and pressure $p(z,t)$, at the depth z and time t are

$$\frac{\rho a^2}{A}\frac{\partial q(z,t)}{\partial z} + \frac{\partial p(z,t)}{\partial t} = 0, \quad (11)$$

$$\frac{A}{\rho}\frac{\partial p(z,t)}{\partial z} + \frac{\partial q(z,t)}{\partial t} + Rq(z,t) - Ag = 0, \quad (12)$$

where g (9.81 m/s^{-2}) is the acceleration due to gravity; A (m^2) is the cross sectional area of the well; $a^2 = K/[\rho + KD\rho(eE)^{-1}]$ (m/s) is the velocity of the water-hammer wave; $R = 32\nu/D^2$ (s^{-1}) is the laminar flow friction effect;, and the remaining parameters are defined in Table 1. Solving the equations in the Laplace domain leads to a hyperbolic equation with two boundary conditions. At each side of the well bore only one of the variables can be the boundary condition, therefore in accordance with the well testing configuration the flow rate at the well head and the pressure at the bottom hole (denoted q_{wh} and p_{bh} respectively) are taken as the boundary conditions. This results in the following equations:

$$\begin{bmatrix}\mathcal{P}_{wh}(s)\\ \mathcal{Q}_{bh}(s)\end{bmatrix} = \mathbb{W}\begin{bmatrix}\mathcal{Q}_{wh}(s)\\ \mathcal{P}_{bh}(s)\end{bmatrix}, \quad (13)$$

where $\mathcal{P}_{wh}(s)$ and $\mathcal{P}_{bh}(s)$ are the Laplace transforms of the pressure at the well head and bottom hole respectively, $\mathcal{Q}_{wh}(s)$ and $\mathcal{Q}_{bh}(s)$ and the Laplace transforms of the flow rate at the well head and bottom hole respectively, and

$$W_{11} = \frac{\rho\mu a^2}{sA}\tanh\mu L \qquad W_{12} = \frac{1}{\cosh\mu L}$$
$$W_{21} = \frac{1}{\cosh\mu L} \qquad W_{22} = -\frac{sA}{\rho\mu a^2}\tanh\mu L.$$

This is the model of the well.

Table 1. Well bore and Reservoir Properties

Model Parameters	Parameter Values
Reservoir boundary, (r_e)	3000 m
Well radius, (r_w)	0.1 m
Reservoir height, (H)	50 m
Pipe internal diameter, (D)	0.1 m
pipe wall thickness,(e)	16×10^{-3}m
Well length, (L)	2000 m
Permeability of rock, (k)	200 mD
Porosity of rock, (ϕ)	0.2
Viscosity of fluid, (μ)	0.01 Pa.s
Total compressibility, (C_t)	7.25×10^{-9} Pa^{-1}
bulk modulus elasticity of the fluid, (K)	1.5×10^{9} Pa
kinematic viscosity of the fluid,(ν)	1.11×10^{-5} m^2 s^{-1}
Density of fluid, (ρ)	900 Kgm^{-3}
Young's Modulus of elasticity, (E)	200×10^{9}Pa

Now consider modeling the reservoir. A reservoir consists of porous rock filled with fluid. The reservoir is modeled as a cylinder, with fluid flowing radially toward the well bore. The outer edge of the reservoir is called the *outer boundary*. The intersection of the well bore and the reservoir is called the *sandface*. In this situation, the radial flow rate $q(r,t)$ and pressure $p(r,t)$ in the reservoir at radial distance r from the symmetry axis, satisfy the diffusivity equation and Darcy's law [Lee, 1982]

$$\frac{1}{r}\frac{\partial}{\partial r}r\frac{\partial p(r,t)}{\partial r} = \frac{1}{\eta}\frac{\partial p(r,t)}{\partial t} \tag{14}$$

$$q(r,t) = -\frac{2\pi rkh}{\mu}\frac{\partial p(r,t)(t)}{\partial r} \tag{15}$$

with $\eta = k/\phi\mu c_t$ is the hydraulic diffusivity; and the remaining parameters are defined in Table 1.

Solution of the elliptic diffusivity equation in the Laplace domain requires two boundary conditions which are chosen to be the flow rate at the sand face and the pressure at the outer boundary (denoted $q_{sf}(t)$ and $p_o(t)$ respectively). This leads to

$$\begin{bmatrix}\mathcal{P}_{sf}(s)\\ \mathcal{Q}_o(s)\end{bmatrix} = \mathbb{R}\begin{bmatrix}\mathcal{Q}_{sf}(s)\\ \mathcal{P}_o(s)\end{bmatrix} \tag{16}$$

in which $\mathbb{R}$ is a 2× 2 matrix with

$$\begin{aligned}
R_{11} &= \frac{\mu}{2\pi khr_w\sqrt{\frac{s}{\eta}}}\frac{I_{0e}K_{0w} - I_{0w}K_{0e}}{I_{0e}K_{1w} + I_{1w}K_{0e}},\\
R_{12} &= \frac{I_{0w}K_{1w} + I_{1w}K_{0w}}{I_{0e}K_{1w} + I_{1w}K_{0e}},\\
R_{21} &= \frac{r_e}{r_w}\frac{I_{1e}K_{0e} - I_{0e}K_{1e}}{I_{0e}K_{1w} + I_{1w}K_{0e}},\\
R_{22} &= \frac{2\pi kh}{\mu}r_e\sqrt{\frac{s}{\eta}}\frac{I_{1w}K_{1e} - I_{1e}K_{1w}}{I_{0e}K_{1w} + I_{1w}K_{0e}}.
\end{aligned} \tag{17}$$

where I and K are modified Bessel functions of the first and second kind and $I_{ij} = I_i(r_j\sqrt{\frac{s}{\eta}})$ and $K_{ij} = K_i(r_j\sqrt{\frac{s}{\eta}})$.

The model of the production system is obtained by concatenating the bottom hole side of the well bore model to the sand face side of the reservoir model by coupling $q_{bh}(t)$ to $q_{sf}(t)$ and $p_{sf}(t)$ to $p_{bh}(t)$ as shown in Figure 7.

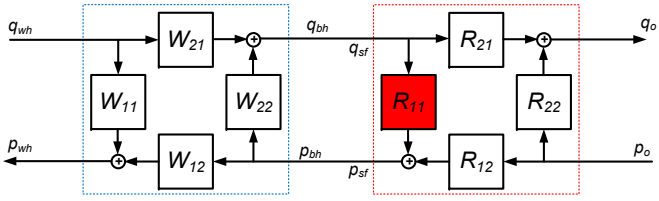

Fig. 7. Bilaterally coupled reservoir and well bore model

From a well test analysis point of view, the parameters are conventionally estimated from R_{11} that we identify.

To this end, we isolate the parts of the network shown in Fig. 7 that are relevant for the identification of R_{11} into the structure that is given in Fig. 8. We have removed R_{12} from the network because it has a very small gain.

4.2 Data generating system

Formulating the corresponding system identification problem for the well test analysis requires using measurement devices in the correct positions in the model. In a typical production setup, (see Figure 6), the wellhead flow rate and the bottom hole pressure and flow rate are measured. Both sensor and process noise are present in the data. The process noise is due to phenomena such as turbulence, sudden well bore reservoir condition change, two phase flow occurrence, etc. It is assumed that the well head measurement does not have process noise. In Figure 8 the model is shown with all measurement devices and noise terms.

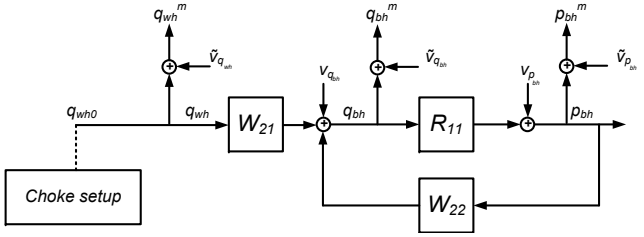

Fig. 8. Bilaterally coupled reservoir/well bore with measurements

The transfer function $R_{11}(z)$ can be identified consistently using the identification methods developed in section 3.1. The estimated transfer function $R_{11}(z,\hat{\theta})$ is then used to obtain an estimate of the permeability k. Let $R_{11}(s,k)$ be a continuous-time model defined by (17) where only k is a free parameter, and all other parameters in (17) are assumed to be known. To compare a continuous-time and discrete-time transfer function it is easiest to move to frequency domain. Thus the estimate of k is found by minimizing the difference between $R_{11}(z,\hat{\theta})$ and $R_{11}(s,k)$:

$$\hat{k} = \arg\min_{k} \frac{1}{M} \sum_{m=1}^{M} \left\| R_{11}(j\omega_m, k) - R_{11}(e^{j\omega_m}, \hat{\theta}) \right\| W(\omega_m) \tag{18}$$

where $W(\omega_l)$ is a user defined weighting function, and ω_1 and ω_M define the frequency range of interest.

5. RESULTS AND DISCUSSION

To simulate the system, the discrete approximation of transfer functions in (13) and (16) are used. The system is excited with a PRBS signal with the clock parameter of 3600 seconds; i.e. the surface choke to be in one state for at least for one hr. Practically it is not feasible to change the surface choke setting too often. Colored process noise of 30 and 34 dB are added to bottom hole flow rate and pressure measurements respectively. White sensor noise of 40, 27, and 40 dB are added to wellhead flow rate, bottom hole flow rate and bottom hole pressure measurements respectively. The SNR of q_{bh} is considered to be the lowest von Schroeter et al. [2004]. A dataset with $N = 500000$ and $T_s = 1$ sec is used. Both the non-parametric and IV methods are applied to the simulated data set. The results are shown in Fig. 9. The high variance of the non-parametric estimate at high frequency is due to the fact that the system is not excited at these frequencies. For the IV estimate the data was resampled by a factor of 9 in order to remove the higher frequency content from the data. In addition low-pass prefilters were used to put extra weighting on the lower frequencies.

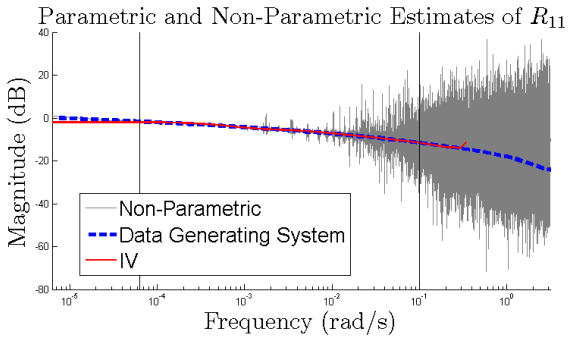

Fig. 9. Parametric and non-parametric estimates of R_{11}

The reservoir module R_{11} has a diffusive behavior which results in a low pass frequency response. The identified model captures this behavior for $\omega = [2\pi \times 10^{-5} - 1 \times 10^{-1}]$ rad/sec. The lower bound is chosen as a rule of thumb to be five times the lowest available measured frequency, and the higher bound is chosen till the frequency which the frequency response shows a smooth behavior. The estimation results for the average permeability k is 199.9 mD which is quite close to the true value.

6. CONCLUSIONS

Bilaterally coupled systems are useful to model many physical systems where there is an exchange of energy. In this paper we have presented an identification method that can be used to identify modules in bilaterally-coupled systems. The method results in consistent estimates even in presence of sensor noise, which is often present in practical situations. The method allows us to use noisy measured data to do well test analysis.

ACKNOWLEDGMENT

Mehdi Mansoori acknowledges D. Rashtchian as his supervisor in Sharif University of Technology and the authors acknowledge J.D. Jansen for the valuable discussion about the modeling section.

REFERENCES

M.H. Chaudhry. *Applied Hydraulic Transients*. Van Nostrand Reinhold Co., New York, 2nd edition, 1987.

A. Dankers, Paul M. J. Van den Hof, Peter S. C. Heuberger, and X. Bombois. Dynamic network structure identification with prediction error methods - basic examples. In *Proceedings of 16th IFAC Symposium on System Identification*, Brussels, Belgium, July 2012.

A.G. Dankers, P.M.J. Van den Hof, X. Bombois, and P.S.C. Heuberger. Predictor input selection for two stage identification in dynamic networks. In *Proceedings of the European Control Conference 2013*, pages 1422–1427, Zurich, Switzerland, July 2013.

U. Forssell and L. Ljung. Closed-loop identification revisited. *Automatica*, 35:1215–1241, 1999.

M. Gilson and P.M.J. Van den Hof. Instrumental variable methods for closed-loop system identification. *Automatica*, 41:241–249, 2005.

A. Gringarten. From straight lines to deconvolution: The evolution of the state of the art in well test analysis. *SPE Reservoir Evaluation Engineering*, 11(1), February 2008.

John Lee. *Well testing*. New York: Society of Petroleum Engineers, 1982.

L. Ljung. *System Identification: Theory for the User*. Prentice-Hall, Englewood Cliffs, NJ, 1999.

D. Materassi and G. Innocenti. Topological identification in networks of dynamical systems. *IEEE Trans. Automatic Control*, 55(8):1860–1871, 2010.

B.M. Sanandaji, T.L. Vincent, and M.B. Wakin. Exact topology identification of large-scale interconnected dynamical systems from compressive observations. In *Proceedings of American Control Conference*, pages 649–656, San Francisco, CA, USA, 2011.

T. Söderström. System identification for the errors-in-variables problem. *Transactions of the Institute of Measurement and Control*, 34:780–792, 2012.

T. Söderström, L. Wang, R. Pintelon, and J. Schoukens. Can errors-in-variables systems be identified from closed-loop experiments. *Automatica*, 49:681–684, 2013.

P.M.J. Van den Hof, A.G. Dankers, P.S.C. Heuberger, and X. Bombois. Identification of dynamic models in complex networks with prediction error methods - basic methods for consistent module estimates. *Automatica*, 49(10):2994–3006, 2013.

T. von Schroeter, F. Hollaender, and A. Gringarten. Deconvolution of well-test data as a nonlinear total least-squares problem. *SPE Journal*, 9(4):375–390, 2004.